Effect of Radiation in Buoyancy Induced Turbulent Flows in Partial Enclosures

By

Suhas Suresh Gaikwad
Roll No. ME14MTECH11013

Under the guidance of
Dr. K.Venkatasubbaiah

A Thesis Submitted
in Partial Fulfillment of the Requirements
for the Degree of
Master of Technology

**Department Of Mechanical And Aerospace Engineering
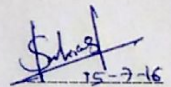Indian Institute Of Technology Hyderabad**

भारतीय प्रौद्योगिकी संस्थान हैदराबाद
Indian Institute of Technology Hyderabad

JULY 2016

Declaration

I declare that this written submission represents my ideas in my own words, and where ideas and words of others have been included, I have adequately cited and referenced the original sources. I also declare that I have adhered to all principles of academic honesty and integrity and have not misinterpreted or fabricated or falsified any idea/data/fact/source in my submission. I understand that any violation of the above will be a cause for disciplinary action by the Institute and can also evoke penal action from the sources that have thus not been properly cited, or from whom proper permission has not been taken when needed.

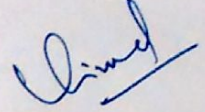(Signature)

Suhas Suresh Gaikwad

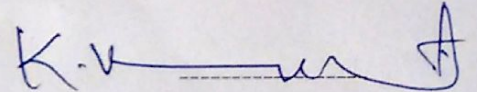(Student Name)

ME14MTECH11013

(Roll No.)

Approval Sheet

This thesis entitled "Effect of Radiation in Buoyancy Induced Turbulent Flows in Partial Enclosures " by Suhas Suresh Gaikwad is approved for the degree of Master of Technology from IIT Hyderabad.
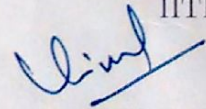
(Dr. Vinod Janardhanan) External examiner
Dept. of Chemical Engg.
IITH

(Dr. Saravanan Balusamy) Internal examiner
Dept. of Mechanical And Aerospace Engg.
IITH

(Dr. K. Venkatasubbaiah) Adviser
Dept. of Mechanical And Aerospace Engg.
IITH

(Dr. Vinod Janardhanan) Chairman
Dept. of Chemical Engg.
IITH

Acknowledgements

I express my sincere gratitude to my thesis supervisor Dr. K. Venkatasubbaiah Associate Professor in the Department of Mechanical and Aerospace Engineering, Indian Institute of Technology Hyderabad for his valuable guidance and encouragement during the course of the work. I am thankful to him for his constant support and timely suggestions during demanding times of the work. I would like to make a special mention of the excellent computational facilities provided by Dr. K. Venkatasubbaiah. Finally, I would like to thank my parents for their constant support and encouragement.

To my family ...

Abstract

This study consists of two parts one aims at incorporating radiation effects of wall in partial enclosure and another being the analysis of train fire with the help of Fire Dynamics Simulator. The flow situation is two dimensional, turbulent natural convection flow. The flow is studied using stream function and vorticity formulation approach with radiation thermal boundary condition. For turbulence the $k - \epsilon$ model of Lam-Bremhorst is used. For the first part the study is carried out for a vented enclosure with heat source placed at center at bottom wall. Conventionally in a given flow situation the boundary conditions are assumed to be adiabatic but the radiation by walls and heat source affects the flow field and temperature field considerably. This study is an attempt to consider the radiation effects and get more realistic results. The computer programming being used to implement the radiation effects is FORTRAN. The study has been carried out for different Grashof numbers varying from 10^8 to 10^{10}, three different materials namely Concrete, Iron and Plaster of Paris. Also the study is carried for two different thicknesses 10 mm and 1 mm. A radiation model is developed first and is then implemented. Fin approach with Radiation-Irradiation formulation was used for developing Radiation model. The validations are done using standard square enclosure with heated and cooled walls as reference cases. The heat transfer characteristics comprising of Effect on temperature profiles, Nusselt number and velocity are reported for above cases. For the second part the study has been carried out for fire in stationary and moving train, results are analysed for these cases. Using this analysis the threat level is reported and safety measures are provided.

Contents

List of Figures

List of Tables

Nomenclature

h Convective heat transfer coefficient (W/m^2K)

H Height of enclosure (m)

W Width of enclosure (m)

D Width of ceiling vent (m)

T_s Heat source temperature

T_w Wall temperature

T_∞ Initial fluid temperature

g Gravitational acceleration (m/s^2)

k Turbulence kinetic energy (m^2/s^2)

K Dimensionless turbulence kinetic energy

Nu Nusselt number

Pr Prandtl number

Pr_t Turbulent prandtl number

Ra Rayleigh number

Gr Grashoff number

Re Reynolds number

T Temperature (K)

t Time (s)

u, v Velocity components in x and y directions

U, V Dimensionless velocity components in x and y directions

W Width of the channel (m)

x, y Cartesian co-ordinates

X, Y Dimensionless scales in x and y directions

ψ Stream function

ω Vorticity

ϵ Turbulence diffusion (m^2/s^3)

β Coefficient of thermal expansion (K^{-1})

ν Kinematic viscosity (m^2/s)

α Thermal diffusivity (m^2/s)

ν_t Turbulent eddy viscosity (m^2/s)

τ Dimensionless time scale

θ Dimensionless temperature

Ω Dimensionless Vorticity

Ψ Dimensionless stream function

E Dimensionless dissipation

K_w Thermal conductivity of wall(W/m K)

K_f Thermal conductivity of fluid(W/m K)

t_w Thickness of wall(m)

C_w Heat capacity of wall(Kj/Kg K)

ρ_w Density of wall material(Kg/m^3)

ϵ_w Emissivity of wall material

α_w Absorptivity of wall material

σ Stefan-Boltzman constant($W/K^4 m^2$)

ΔT $(T_s - T_\infty)$

B Radiosity matrix

G Irradiation matrix

TEM Temperature matrix on RHS

SFM Shape factor matrix

$CONSTM$ Constant matrix

Nu_c Convective Nusselt number

Nu_r Radiative Nusselt number

Chapter 1

Introduction

Heat transfer by free convection in partial enclosure with radiation effects is an important practical case in many engineering applications like solar collectors, design of building with thermal comfort, electronic equipments etc. Heat transfer from an object to another object happens either with conduction, convection and radiation or combination of these modes. Conduction is a mode of heat transfer which occurs when there is temperature gradient in stationary medium (solid or fluid). Convection is mode of heat transfer which occurs between a surface and relatively moving fluid. The radiation occurs just by virtue of surface temperature. Convection is further divided into two types forced convection and natural convection. In this study we will be dealing with the free or natural convection. The natural convection flow is also called as buoyancy driven flow. The density differences in the different layers of the fluid along with the effect of gravity, forces heavier molecules downwards and lighter molecules upwards leading to buoyancy driven flow. The difference in density may be due to following reasons namely temperature difference, multiple phases present in the fluid and difference in concentration of chemical species. Here we will be studying the natural convection due to temperature difference. These flows are further divided as vertical flow and horizontal flow. Numerous studies have been done on natural convection flows. A numerical study of 3-D natural convection flows in a rectangular cavity was carried out for a steady state laminar flow [1]. In a study benchmark numerical solution for a natural convection flow in a square cavity was provided [2]. A study involved investigation of the effect of changing thermal boundary condition on the flow field in natural convection flow inside square cavity [3]. These studies were carried out for laminar flows. Also, Laminar and turbulent natural convection was numerically studied [4] in a square cavity with differentially heated side walls a bench-

mark case i.e. isothermal side walls using $k - \epsilon$ turbulence model. The experimental study was also done involving the low turbulence natural convection flow field inside square cavity and provided thermal plots and flow vectors [5]. The numerical study of buoyancy driven flow in a square cavity with differentially heated vertical walls and adiabatic horizontal walls for Ra= 10^7 using lattice Boltzmann method was carried out [6]. Another study involving the turbulent natural convection flows inside a rectangular enclosure was carried out considering the conduction along the thickness of the wall and reported a correlation for average Nusselt number in terms of Grashof number [7]. There were studies involving both the laminar and turbulent flows inside square enclosure with $k - \epsilon$ turbulence model [8]. But, the above cases involved the flow study inside a closed enclosure which does not represent a practical model. The more practical case of natural convection flow involves flow inside an enclosure with vent at its ceiling. Not much has been studied for this case. A few papers are available for this case. Numerical investigation of a 2D, laminar flow inside a partial enclosure has been done [9]. Stream function vorticity formulation was used with Boussinesq approximation . Experimental studies were carried out investigating the fire induced flows through an opening such as window or door [10]. A more practical case of fire induced turbulent flow inside a partial enclosure was studied [11, 12]. In this study flow inside a partial enclosure was modeled as 2-D, incompressile, turbulent flow where turbulence was modeled with $k - \epsilon$ model of Lam Bremhorst. Heat source and vent are centrally located with equal width. The thermal boundary conditions used for the study were adiabatic for all walls except the heat source. To sum up all the above cases were studied without considering radiation effects of the wall surface. So it was important to carry out a study involving much more practical case. Present work is a extension of this work with radiation effects. These vented enclosures are studied here with radiation boundary condition. In general walls of the a enclosure are treated as adiabatic where heat transfer is neglected. This study primarily aims at taking radiation effects into account of such walls. The cases that are studied consists of higher values of Grashof number ($Gr > 10^8$) hence turbulence comes into picture. One of the important aspect of analyzing natural convection flows is modeling of turbulence. The $k - \epsilon$ model of Lam-Bremhorst is used in present study. So this study involves buoyancy induced, two dimensional, unsteady, incompressible, turbulent flow in an partial enclosure considering radiation effects and using $k - \epsilon$ model of Lam Bremhorst for modeling turbulence with Boussinesq framework.

1.1   Literature survey

There have been several studies done for analyzing flow inside a enclosure. Based on whether the flow is laminar or turbulent, inside a square enclosure or a rectangular enclosure, inside a inclined enclosure, horizontal flow or vertical flow for various aspect ratios numerous papers have been published as discussed in the introductory part.

To come up with taking the case of turbulent natural convection with radiation in a partial enclosures for the study so many papers helped. Experimental study of natural convection inside square enclosure with radiation effects was studied by Ramesh *et al.* [13] in laminar range using differential interferometer and reported significant change in flow pattern and heat transfer characteristics. Extensive study involving interaction effects of surface radiation on turbulent natural convection in square and rectangular enclosures with isothermal adiabatic walls was carried out by Velusamy *et al.* [14]. The results were reported for wide range of Rayleigh numbers ranging from 10^9 to 10^{12} and for aspect ratios 1 to 200. The approach used to include surface radiation effects was steady state fin approach with radiation irradiation formulation. They have reported higher velocity and turbulence levels as a result of interaction of surface radiation there by increasing the convective Nusselt number. Singh *et al.* [15] studied steady state natural convection flow with radition inside side vented open cavities. Bouali *et al.* [16] studied the effects of surface radiation in an inclined rectangular enclosure with a inner body kept at its center. The flow condition is 2-D,laminar, incompressible flow in a rectangular enclosure of A.R.= 2 with isothermal vertical walls. The approach used for modeling radiation was radiative flux approach without considering the conduction effects. They reported the effect of inclination on heat transfer and dependence of inner body thermal conductivity on inclination angle. Lauriat *et al.* [17] studied the effect of surface radiation on conjugate natural convection in partial enclosures. A rectangular enclosure with cold external ambient and hot internal ambient with vents on vertical wall was studied. The radiative flux approach was used to model radiation. Sharma *et al.* [18] studied conjugate turbulent natural convection with surface radiation in a rectangular enclosure with transparent medium. A typical case with heated bottom wall and cooled from other walls resembling Liquid Metal Fast Breeder Reactor was studied. The flow was modeled as 2-D, incompressible, turbulent flow with standard two equation $k - \epsilon$ model for modeling turbulence. The steady state fin approach with radiation irradiation formulation was used for modeling radiation. A correlation for the mean convective Nusselt number in terms of Rayleigh number and aspect ratio along with the effect of emissivity on heat transfer was reported. Singh *et al.* [19] studied the

case of free convection with surface radiation in open top cavity. The approach used for the study was steady state fin approach for modeling radiation. They reported the location of heat source for effective cooling of the room at top left position. Hinojosa *et al.* [20] reported convective and radiative Nusselt numbers for flow inside tilted cavity.

1.2 Motivation

There have been several studies for buoyancy driven turbulent flows in square and rectangular enclosures with and without radiation model.But a more realistic and practical case of enclosure i.e enclosure with vent and heat source at bottom which very much resembles to the fire induced flow in buildings is less studied. With reference to [11] the above case is studied but assuming adiabatic wall boundary condition. So this study is an attempt to analyze a more practical case of vented enclosure considering radiation effects.The steady state fin approach was used in analyzing flow inside square and rectangular enclosures earlier. In this study for the first time a unsteady state radiation model is developed and used for analysis.

1.3 Objectives

Objective of the present study is to find out the effect of radiation in an partial enclosure with turbulent natural convection flow. Various objectives of the study are enumerated as following

- To develop a radiation model to account the surface radiation effects.

- To study the effects of inclusion of surface radiation on heat transfer characteristics in a square enclosure.

- To study the effects of inclusion of surface radiation on heat transfer characteristics and flow structures in a partial enclosure.

- To study the effect of Grashof number on flow behavior and heat transfer characteristics in a partial enclosure.

- To study the effect of thickness on flow behavior and heat transfer characteristics in a partial enclosure.

- To study the effect of material on flow behavior and heat transfer characteristics in a partial enclosure

1.4   Outline of thesis

In this thesis, the effects of radiation in a buoyancy driven turbulent flow in a partial enclosure is studied numerically. For a range of Grashoff number, thickness of the wall and wall materials the study has been carried out and results have been reported.

- Chapter 1 provides an introduction to the topic, literature survey, motivation and gives the outline of thesis.

- Chapter 2 discusses the governing equations, initial and boundary conditions for convection and radiation parts.

- Chapter 3 provides information on the numerical methods used to solve governing equations.

- Chapter 4 explains the results and discussions.

- Chapter 5 deals with a new topic of train fire analysis using fire dynamic simulator.

- Chapter 6 summarizes the conclusions obtained from the study.

Chapter 2

Governing equations and Initial & Boundary conditions

2.1 For Natural convection

The flow inside a square enclosure with vent at ceiling and heat source placed at bottom is as shown in the figure.2.1. The width of the ceiling vent and heat source is D. The width of the enclosure is H. The ambient temperature at initial condition is T_∞ and heat source temperature is T_s. The Grashof number based on width involved in the study are above 10^6 which makes the flow inside enclosure turbulent. In order to solve turbulent flows numerically, we have three approaches namely Reynolds Averaged Navier Stokes Equation (RANS), Large Eddy Simulations(LES) and Direct Numerical Simulations(DNS). RANS equations are time averaged equations of motion of fluid flow. Here an instantaneous quantity is decomposed into time averaged and fluctuating quantity. LES approach ignores the smallest length scales involved in solving Navier Stokes equation. This is done to reduce the requirement of large computational power which increases computational cost to a great extend. DNS method directly solves the Navier Stokes equations numerically without any turbulence model which involves wide range of time and length scales. This means from the smallest spatial scales(Kolmogorov scales) to the largest scales of integral scale has to be resolved on computational domain.It involves higher memory storage capacity and hence not suitable for the present study. Out of these methods RANS equations with suitable turbulence model is used in this study.
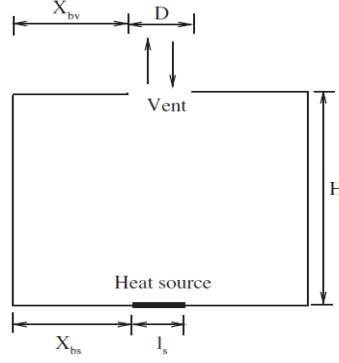
Figure 2.1: Schematic diagram of partial enclosure used in study

RANS equations as discussed are formed by time averaging the Navier Stokes equations in which instantaneous quantities like velocity, temperature and pressure are taken as a sum of time averaged and fluctuating quantities. For our case of 2-D, incompressible flow we get four governing equations namely time averaged continuity equation, time averaged x momentum equation, time averaged y momentum equation and time averaged energy equation for mean temperature field. Because of time averaging three extra terms are created in momentum equation called as Reynold's stresses and two in energy equation. So we now have 9 unknowns and 4 equations. In order to resolve this closure problem of turbulence we use Boussinesq hypothesis with $k - \epsilon$ model. This flow situation has been extensively studied and it was suggested that the more suitable model for turbulence is $k - \epsilon$ model of Lam Bremhorst [11, 12]. Same governing equations are used in this study as given below.

$$\frac{\partial u}{\partial x} + \frac{\partial v}{\partial y} = 0 \tag{2.1}$$

$$\frac{\partial u}{\partial t} + u\frac{\partial u}{\partial x} + v\frac{\partial u}{\partial y} = -\frac{1}{\rho}\frac{\partial p}{\partial x} + v\left[\frac{\partial^2 u}{\partial x^2} + \frac{\partial^2 u}{\partial y^2}\right] + 2\frac{\partial}{\partial x}\left[v_t\frac{\partial u}{\partial x}\right] + \frac{\partial}{\partial y}\left[v_t\frac{\partial u}{\partial y}\right] + \frac{\partial}{\partial y}\left[v_t\frac{\partial v}{\partial x}\right] \tag{2.2}$$

$$\frac{\partial v}{\partial t} + u\frac{\partial v}{\partial x} + v\frac{\partial v}{\partial y} = -\frac{1}{\rho}\frac{\partial p}{\partial y} + v\left[\frac{\partial^2 v}{\partial x^2} + \frac{\partial^2 v}{\partial y^2}\right] + \frac{\partial}{\partial x}\left[v_t\frac{\partial u}{\partial y}\right] + \frac{\partial}{\partial x}\left[v_t\frac{\partial v}{\partial x}\right] + 2\frac{\partial}{\partial y}\left[v_t\frac{\partial v}{\partial y}\right]$$
$$+ \mathrm{g}\beta(T - T_\infty), \tag{2.3}$$

$$\frac{\partial T}{\partial t} + u\frac{\partial T}{\partial x} + v\frac{\partial T}{\partial y} = \frac{\partial}{\partial x}\left[\left(\alpha + \frac{v_t}{Pr_t}\right)\frac{\partial T}{\partial x}\right] + \frac{\partial}{\partial y}\left[\left(\alpha + \frac{v_t}{Pr_t}\right)\frac{\partial T}{\partial y}\right], \tag{2.4}$$

$$\frac{\partial k}{\partial t} + u\frac{\partial k}{\partial x} + v\frac{\partial k}{\partial y} = \frac{\partial}{\partial x}\left[\left(v + \frac{v_t}{\sigma_k}\right)\frac{\partial k}{\partial x}\right] + \frac{\partial}{\partial y}\left[\left(v + \frac{v_t}{\sigma_k}\right)\frac{\partial k}{\partial y}\right] - \frac{g\beta v_t}{Pr_t}\frac{\partial T}{\partial y} - \epsilon$$
$$+ v_t\left[2\left(\frac{\partial u}{\partial x}\right)^2 + 2\left(\frac{\partial v}{\partial y}\right)^2 + \left(\frac{\partial u}{\partial y} + \frac{\partial v}{\partial x}\right)^2\right], \tag{2.5}$$

$$\frac{\partial \epsilon}{\partial t} + u\frac{\partial \epsilon}{\partial x} + v\frac{\partial \epsilon}{\partial y} = \frac{\partial}{\partial x}\left[\left(v + \frac{v_t}{\sigma_\epsilon}\right)\frac{\partial \epsilon}{\partial x}\right] + \frac{\partial}{\partial y}\left[\left(v + \frac{v_t}{\sigma_\epsilon}\right)\frac{\partial \epsilon}{\partial y}\right] - C_{2\epsilon}f_2\frac{\epsilon^2}{k}$$
$$+ C_{1\epsilon}f_1\left[v_t\left\{2\left(\frac{\partial u}{\partial x}\right)^2 + 2\left(\frac{\partial v}{\partial y}\right)^2 + \left(\frac{\partial u}{\partial y} + \frac{\partial v}{\partial x}\right)^2\right\}\right] - C_{3\epsilon}\frac{g\beta v_t}{Pr_t}\frac{\partial T}{\partial y} \tag{2.6}$$

The fire induced turbulent flow inside the enclosure is modeled as the unsteady state, incompressible buoyancy driven turbulent flow. The governing equations for this type of flow consists of Reynolds Averaged Navier-Stoke equations (RANS), time averaged energy equation for mean temperature field. The Boussinesq approximation is used for modeling of buoyancy term. Value of density is taken as constant for all equations except momentum equations. $k - \epsilon$ model of Lam Bremhorst is used for modeling turbulence. The contribution of the buoyancy force in turbulent kinetic energy generation and dissipation is considered.

The non dimensional form of governing equations are obtained by the following non dimensional variables.

$$X = \frac{x}{L}; Y = \frac{y}{H}; U = \frac{u}{V_c}; V = \frac{v}{V_c}; \tau = \frac{tV_c}{H}; \theta_f = \frac{T - T_\infty}{T_s - T_\infty}; V_c = \sqrt{g\beta\Delta TH};$$

$$\Omega = \omega\sqrt{\frac{H}{g\beta\Delta T}}; \Psi = \frac{\psi}{\sqrt{g\beta\Delta TH^3}}; K = \frac{k}{g\beta\Delta TH}; \varepsilon = \frac{\epsilon}{\sqrt{(g\beta\Delta T)^3 H}}$$

The non-dimensional form of the governing equations are as follows:

$$\frac{\partial^2 \Psi}{\partial X^2} + \frac{\partial^2 \Psi}{\partial Y^2} = -\Omega, \tag{2.7}$$

$$\frac{\partial \Omega}{\partial \tau} + U\frac{\partial \Omega}{\partial X} + V\frac{\partial \Omega}{\partial Y} = \frac{\partial^2}{\partial X^2}\left[\left(\frac{1}{(\mathrm{Gr})^{1/2}} + \frac{1}{\mathrm{Re}_t}\right)\Omega\right] + \frac{\partial \theta}{\partial X} + \frac{\partial^2}{\partial Y^2}\left[\left(\frac{1}{(\mathrm{Gr})^{1/2}} + \frac{1}{\mathrm{Re}_t}\right)\Omega\right]$$
$$+ 2\frac{\partial U}{\partial Y}\frac{\partial^2}{\partial X^2}\left[\frac{1}{\mathrm{Re}_t}\right] - 2\frac{\partial V}{\partial X}\frac{\partial^2}{\partial Y^2}\left[\frac{1}{\mathrm{Re}_t}\right] + 2\left[\frac{\partial V}{\partial Y} - \frac{\partial U}{\partial X}\right]\frac{\partial^2}{\partial X\partial Y}\left[\frac{1}{\mathrm{Re}_t}\right], \tag{2.8}$$

$$\frac{\partial \theta}{\partial \tau} + U\frac{\partial \theta}{\partial X} + V\frac{\partial \theta}{\partial Y} = \frac{\partial}{\partial X}\left[\left(\frac{1}{Pr_t(\mathrm{Gr})^{1/2}} + \frac{1}{Pr_t\mathrm{Re}_t}\right)\frac{\partial \theta}{\partial X}\right] + \frac{\partial}{\partial Y}\left[\left(\frac{1}{Pr_t(\mathrm{Gr})^{1/2}} + \frac{1}{Pr_t\mathrm{Re}_t}\right)\frac{\partial \theta}{\partial Y}\right],$$

(2.9)

$$\frac{\partial K}{\partial \tau} + U\frac{\partial K}{\partial X} + V\frac{\partial K}{\partial Y} = \frac{\partial}{\partial X}\left[\left(\frac{1}{(\mathrm{Gr})^{1/2}} + \frac{1}{\sigma_k\mathrm{Re}_t}\right)\frac{\partial K}{\partial X}\right] + \frac{\partial}{\partial Y}\left[\left(\frac{1}{(\mathrm{Gr})^{1/2}} + \frac{1}{\sigma_k\mathrm{Re}_t}\right)\frac{\partial K}{\partial Y}\right]$$
$$- \frac{1}{\mathrm{Re}_t Pt_t}\frac{\partial \theta}{\partial Y} - E + \frac{1}{\mathrm{Re}_t}\left[2\left(\frac{\partial U}{\partial X}\right)^2 + 2\left(\frac{\partial V}{\partial Y}\right)^2 + \left(\frac{\partial U}{\partial Y} + \frac{\partial V}{\partial X}\right)^2\right],$$

(2.10)

$$\frac{\partial E}{\partial \tau} + U\frac{\partial E}{\partial X} + V\frac{\partial E}{\partial Y} = \frac{\partial}{\partial X}\left[\left(\frac{1}{(\mathrm{Gr})^{1/2}} + \frac{1}{\sigma_\epsilon\mathrm{Re}_t}\right)\frac{\partial E}{\partial X}\right] + \frac{\partial}{\partial Y}\left[\left(\frac{1}{(\mathrm{Gr})^{1/2}} + \frac{1}{\sigma_\epsilon\mathrm{Re}_t}\right)\frac{\partial E}{\partial Y}\right]$$
$$+ C_{1\epsilon}f_1\left[\frac{1}{\mathrm{Re}_t}\left\{2\left(\frac{\partial U}{\partial X}\right)^2 + 2\left(\frac{\partial V}{\partial Y}\right)^2 + \left(\frac{\partial U}{\partial Y} + \frac{\partial V}{\partial X}\right)^2\right\} - C_{2\epsilon}f_2\frac{E^2}{K}$$
$$+ C_{3\epsilon}\left\{-\frac{1}{\mathrm{Re}_t Pr_t}\frac{\partial \theta}{\partial Y}\right\}\frac{E}{K}\right]$$

(2.11)

Where the values of constants used for k- ϵ model of Lam Bremhorst are :

$C_\mu = 0.09$; $C_{1\epsilon} = 1.44$; $C_{2\epsilon} = 1.92$; $C_{3\epsilon} = 0.7$; $Prt = 0.9$; $\sigma_k = 1.0$; $\sigma_s = 1.3$.

2.1.1   Initial and Boundary conditions

Initially the non dimensional temperature is taken zero in the whole domain except heat source. Also, the values of k and ϵ are set as numerical zero for all internal points. At boundary the kinetic energy is taken as zero and dissipation follows $\frac{\partial \epsilon}{\partial n} = 0$ At the vent the horizontal velocity is kept zero and vertical velocity follows $\frac{\partial v}{\partial y} = 0$. The temperature of the air leaving vent follows $\frac{\partial T}{\partial y} = 0$. The normal gradients of kinetic energy and dissipation are taken as zero at the vent . At the solid wall no slip condition is taken. Temperature of solid wall is governed by radiation boundary condition which will be discussed in detail in subsequent section. The initial and boundary conditions are given as:

For $\tau = 0$

$\psi = Constant \quad \Omega = \theta = 0$;

For $\tau > 0$

$X = 0; \quad X = 1; \quad 1 > Y > 0 \quad ; \psi = constant;$
$\Omega = -\frac{\partial^2 \psi}{\partial X^2}; \quad \theta = Radiation$
$K = 0; \quad \frac{\partial E}{\partial X} = 0$
$Y = 0; \quad 1 > X > 0 \; ; \psi = constant$
$\Omega = -\frac{\partial^2 \psi}{\partial Y^2}; \quad K = 0; \quad \frac{\partial E}{\partial Y} = 0$
$Y = 0; \quad X_{hs} + D < X < X_{hs}; \quad \theta = radiation$
$Y = 0 \; ; \quad X_{hs} + D > X > X_{hs}; \quad \theta = 1.0$
$Y = 1.0 \; ; \quad X_v > X > X_v + D \quad ; \psi = constant;$
$\Omega = -\frac{\partial^2 \psi}{\partial Y^2}; \quad K = 0; \quad \frac{\partial E}{\partial Y} = 0$
$Y = 1.0 \; ; \quad X_v < X < X_v + D \quad ; \frac{\partial \psi}{\partial Y} = \frac{\partial \Omega}{\partial Y} = \frac{\partial \theta}{\partial Y} = \frac{\partial K}{\partial Y} = \frac{\partial E}{\partial Y} = 0 \; ;$

2.2 Radiation model

2.2.1 Assumptions involved in the radiation model

The assumptions involved in the forming of radiation model are:

- Material of the wall is Isotropic and homogeneous i.e. The values of thermal conductivity, density, Heat capacity, emissivity are constant over all spatial points in the domain.

- The exterior surface of the wall does not take part in radiation. i.e. No irradiation and emission from the exterior surface.

- The heat conduction in wall is along only one direction i.e. 1-D heat conduction.

- The surface of the wall is gray, opaque and diffuse.

- The participating medium is transparent or the medium which does not take part in the radiation phenomenon e.x. air.

- Stefan-Boltzman's law is applicable assuming the wall temperature to be constant and equal to average temperature.

2.2.2 Fin approach

The approach used for developing a radiation model is fin approach. In this approach we consider wall to be a fin and apply governing equation of fin. The wall of the enclosure is considered as a fin which includes the energy interaction by means of conduction, convection and radiation. We write energy balance for the fin considering heat conduction in only one direction (length direction). After deriving the governing equation for the radiation which comes out to be a partial differential equation (PDE), we solve it to include radiation effects of the wall. The governing equation to include radiation effects is formed by writing energy balance for the wall. Let us consider a small element of the wall and writing energy balance considering heat into the system due to conduction, convection and radiation equal to the rate of rise in internal energy of the system. Considering a small element on the wall surface as shown in the figure.2.2.2 and let Q_s be the heat conducted in, Q_{s+ds} be the heat conducted out, q_2 be the heat convected in. ϵG_2 be the absorbed irradiation. Where ϵ_w is the emissivity of the wall surface.
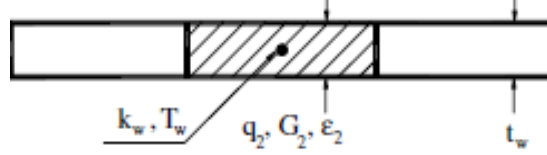

Figure 2.2: Element of the wall

Applying the energy balance we get the following equation:

$$Q_s - Q_{s+ds} + q_2 + \epsilon_w G_2 ds dy - \epsilon_w \sigma T_w^4 ds dy = \frac{\partial (I.E)}{\partial t} \tag{2.12}$$

On solving this, equation becomes

$$t_w K_w \frac{\partial^2 T_w}{\partial s^2} + K_f \frac{(T - T_w)}{\Delta n} + \epsilon_w G_2 - \epsilon_w \sigma T_w^4 = \rho_w t_w C_w \frac{\partial T_w}{\partial t} \tag{2.13}$$

This is the final governing equation for radiation. In order to get wall temperature this equation is solved instead of conventional adiabatic boundary condition. On non dimensionalization the equation becomes:

$$A \frac{\partial^2 \theta_w}{\partial S^2} + B \frac{(\theta - \theta_w)}{\Delta n} + C = \sqrt{Gr} \frac{\partial \theta_w}{\partial \tau} \tag{2.14}$$

Where the non dimensional constants are:

$A = \frac{K_w}{\rho_w C_w \nu};$ $B = \frac{K_f H^2}{\rho_w C_w \nu \Delta n t_w};$ $C = \frac{\epsilon_w K_f H^2}{\rho_w C_w \nu (T_s - T_\infty) t_w} (G_2 - \sigma T_w^4)$

The Non dimensional form of equation is discretized by Forward time Central Space (FTCS) scheme explicitly. The temperature at current time level is dependent on the temperature field at previous level (explicit method) and all the terms are known at previous time level. Then the values of temperature are updated.

2.2.3 Radiation-Irradiation formulation

From the governing equation for radiation formulation we can notice that the only unknown term is irradiation on the wall G_2. We use Radiation-Irradiation formulation for calculating G_2 on each wall.for any gray diffuse surface absorptivity is equal to emissivity from kirchoff's law

$$\alpha_w = \epsilon_w \tag{2.15}$$

Now, Radiosity from the wall surface is given by addition of reflected and emitted radiations

$$B = \epsilon_w \sigma T_{wi}^4 - (1 - \epsilon_{wi})G_{2i} \tag{2.16}$$

Where, i denotes the index of the wall. Now for the whole enclosure irradiation on a wall is addition of fraction of radiosities falling on that wall from all the walls given by

$$G_{2i} = \sum F_{ij} B_j \tag{2.17}$$

Combining equations 2.16 and 2.17 we get equation of the form

$$\sum \frac{(\delta_{ij} - (1 - \epsilon_{wi}) F_{ij}) B_i}{\epsilon_i} = \sigma T_{wi}^4 \tag{2.18}$$

Where, temperature on the right hand side is average wall temperature and F_{ij} is the shape factor or view factor. Writing above equation in the matrix form for all the walls

$$[CONSTM][B] = \sigma \epsilon_{wi} T_{wi}^4 \tag{2.19}$$

Where $CONSTM$ is a constant matrix calculated only once and depends on wall emissivities and shape factors. B is the radiosity matrix and the matrix on the right hand side is emitted radiation matrix.

For six walls and assuming emissivity of all the walls to be equal the constant matrix is given as

$$(1 - \epsilon_w) \begin{pmatrix} 1/(1-\epsilon_w) & F_{12} & F_{13} & F_{14} & F_{15} & F_{16} \\ F_{21} & 1/(1-\epsilon_w) & F_{23} & F_{24} & F_{25} & F_{26} \\ F_{31} & F_{32} & 1/(1-\epsilon_w) & F_{34} & F_{35} & F_{36} \\ F_{41} & F_{42} & F_{43} & 1/(1-\epsilon_w) & F_{45} & F_{46} \\ F_{51} & F_{52} & F_{53} & F_{54} & 1/(1-\epsilon_w) & F_{56} \\ F_{61} & F_{62} & F_{63} & F_{64} & F_{65} & 1/(1-\epsilon_w) \end{pmatrix}$$

Now the shape factors are calculated using Hottel's crossed string method [21] and enclosure theorems. For two parallel surfaces with infinite width this method is applicable. The shape factor of one surface with respect two other is calculated as shown in the figure.2.2.3
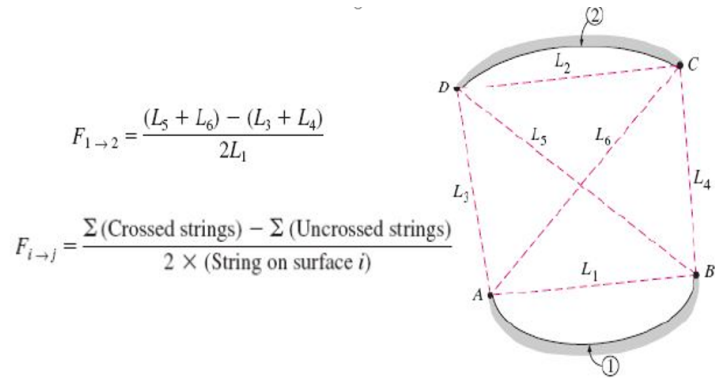
Figure 2.3: Shape factor using Hottel's crossed string method

Shape factors obtained for square enclosure considering four walls are as follows

$$F_{ij} = \begin{pmatrix} 0 & 0.2929 & 0.4142 & 0.2929 \\ 0.2929 & 0 & 0.2929 & 0.4142 \\ 0.4142 & 0.2929 & 0 & 0.2929 \\ 0.2929 & 0.4142 & 0.2929 & 0 \end{pmatrix}$$

Shape factors obtained for vent enclosure considering six walls are as follows

$$F_{ij} = \begin{pmatrix} 0 & 0.1625 & 0.2929 & 0.0891 & 0.1625 & 0.2929 \\ 0.2929 & 0 & 0.1615 & 0.05545 & 0.076 & 0.4141 \\ 0.40625 & 0.40375 & 0 & 0 & 0 & 0.19 \\ 0.4455 & 0.2772 & 0 & 0 & 0 & 0.2772 \\ 0.426 & 0.19 & 0 & 0 & 0 & 0.4037 \\ 0.2929 & 0.4141 & 0.076 & 0.05545 & 0.1615 & 0 \end{pmatrix}$$

Chapter 3

Numerical methods

The governing equations of buoyancy driven turbulent flow are discretized using finite difference schemes. The stream function equation is discretized by second order central difference scheme i.e CD2. Bi-conjugate gradient iterative method is used for solving stream function equation. In the vorticity transport equation (VTE), Energy equation (EE), Kinetic energy equation (KEE) and dissipation equation the diffusion term is discretized by central difference scheme (CD2). The non linear Convection terms are discretized by high accuracy compact schemes which is explained in detail in [22, 23]. The time integration is done using four stage Runge-Kutta Method (RK4). The time step chosen for the study is small $\Delta\tau = 10^{-4}$, which is kept constant for all the simulations. The time step is kept small to avoid divergence of the solution. The parameters are defined using double precision so as to reduce round off errors.

The non dimensional form of the governing equation for radiation is explicitly discretized by forward time central space scheme (FTCS). The non dimensional wall temperature at current time level depends on the temperature field at previous time, hence values of the wall temperatures are updated for every time step. Grid sizes selected for the study were $150 \times 150, 200 \times 200$ for enclosure with vent and $200 \times 100, 100 \times 100$ for square enclosure. Total time required for running a typical vent case simulation with grid size 200×200 was 480 hours and for 150×150 it was 290 hours.

Chapter 4

Results and discussions

In this study as the heat transfer from and to wall surface involves conduction, convection and radiation the non dimensional numbers representing heat transfer are convective Nusselt number and radiative Nusselt number. The local convective Nusselt number on a wall whose length is along X and thickness along Y is the ratio of heat convected from the wall (Q_c) to the heat conducted Q_{cond} calculated as given in equation 4.1.

$$Nu_c = \frac{Q_c}{Q_{cond}}$$
$$Nu_c = \frac{K_f \frac{\partial(T-T_w)}{\partial Y}}{K_f(T_s - T_w)}$$
$$Nu_c = \frac{\partial \Theta}{\partial Y} \tag{4.1}$$

The average convective Nusselt is calculated by integrating these local Nusselt number values over length of wall under consideration by trapezoidal rule. Radiative Nusselt number is the ratio of radiative heat transfer to the conductive heat transfer given by equation 4.2

$$Nu_r = \frac{Q_r H}{K_f(T_s - T_\infty)} \tag{4.2}$$

Where, Q_r is radiative flux received by the wall given by $Q_r = (G - B)$ [20]. For a given wall as the values of irradiation and radiosity are constant for each time step the value of radiative Nusselt number is also constant and hence local radiative Nusselt number is equal to average radiative Nusselt number.

4.1   Validations and Grid independence

For a standard case of square enclosure with horizontal flow or the enclosure with isothermal vertical walls with temperatures T_h and T_c, the code has been validated. Two different cases were studied with $Ra = 10^7$ and $Ra = 10^8$ and average Nusselt numbers were compared. For $Ra = 10^7$ the average hot wall Nusselt number with pure convection without radiation was 16.79 which was well matching with the data from the study carried out by Dixit et al. [6]. Similarly for $Ra = 10^8$ average Nusselt number was compared to the results of Dixit and Babu and Markatos et al. [4]. Also, the mid height non dimensional temperature is plotted for $Ra = 10^7$ and is compared with the results of Dixit et al. [6] as shown in the fig.4.1.
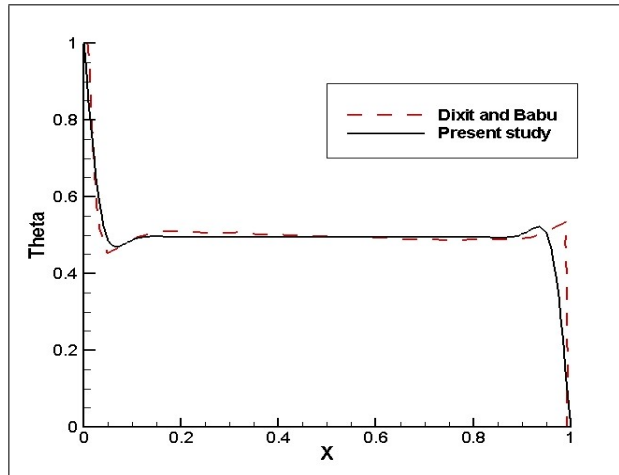
Figure 4.1: Non dimensional temperature at mid height

Average Nusselt number values for these cases have been tabulated as shown in the table 4.1. The results are well matching with the benchmark results.

Table 4.1: Average Nusselt number on the heated wall for square enclosure

Ra	Dixit and Babu [6]	Markatos and Pericleous [4]	Present study
10^7	16.790	-	16.6657
10^8	30.506	32.045	30.57

For grid independence two different grid sizes were selected for the study 200×100 and 100×100. The streamline contours and temperature contours have been plotted for the same as shown in the fig. 4.2 and 4.3.
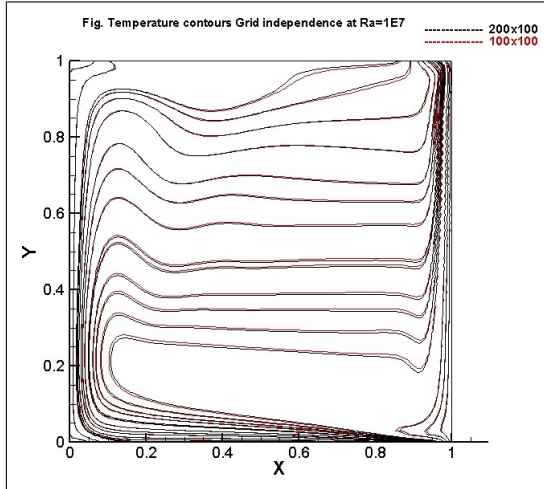
Figure 4.2: Temperature contour for grid independence.
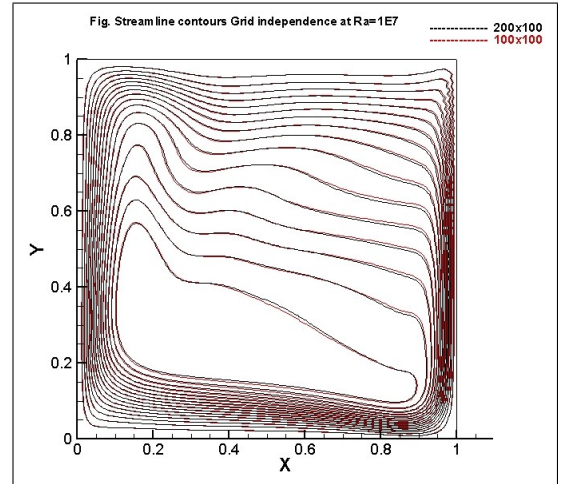
Figure 4.3: Streamline contour for grid independence.

4.2   Results for square enclosure

The mid height non dimensional temperature for $Ra = 10^7$ along the horizontal for pure convection and convection with radiation has been plotted as shown in the figure. The thickness of the wall is 10 mm and material is Iron. 4.4. From the figure it is evident that the temperatures with the surface radiation interaction are lesser. It is because there is increase in heat transfer rate when the surface radiation is accounted.
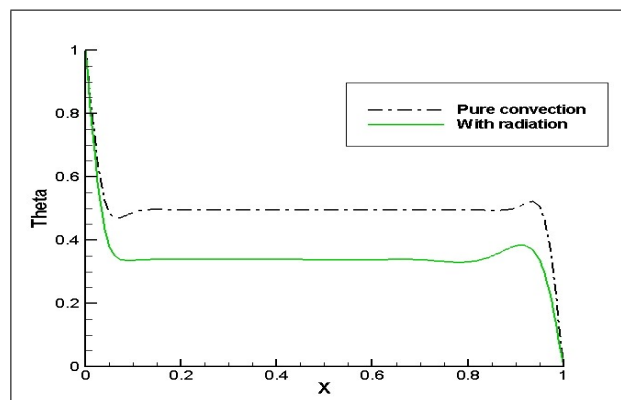
Figure 4.4: Non dimensional temperature at mid height for $Ra = 10^7$

It is found that the top wall temperatures are lesser and bottom wall temperatures are higher in case of convection with surface radiation as compared to pure convection.

Because of this there is variation in local Nusselt number along heated wall as shown in the figure. 4.5. The average Nusselt obtained with the convection is 16.6657 and with the surface radiation effect it is 18.3445. The increase in convective heat transfer is because of the interaction of surface radiation which further increases velocity and turbulence levels in the boundary layers. At corners the convective Nusselt number is lesser for the convection with the surface radiation interaction. It is due to the conduction phenomenon.
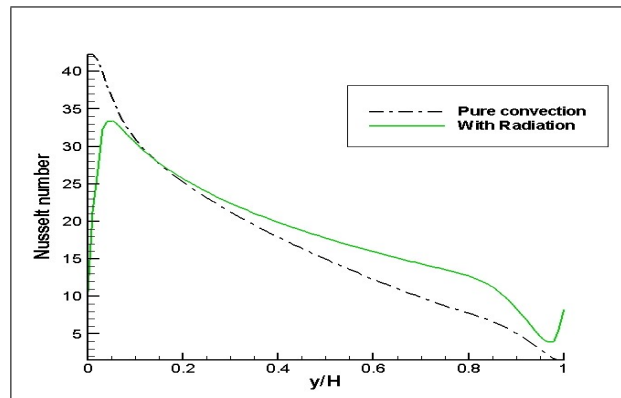
Figure 4.5: Local Nusselt number variation along heated wall for $Ra = 10^7$

Also, similar trend is seen in the local Nusselt number variation on the heated wall for $Ra = 10^8$ as shown in the figure. 4.6. The average value of the Nusselt number over hot wall for convection with radiation is 31.74 whereas for pure convection it is 30.57.
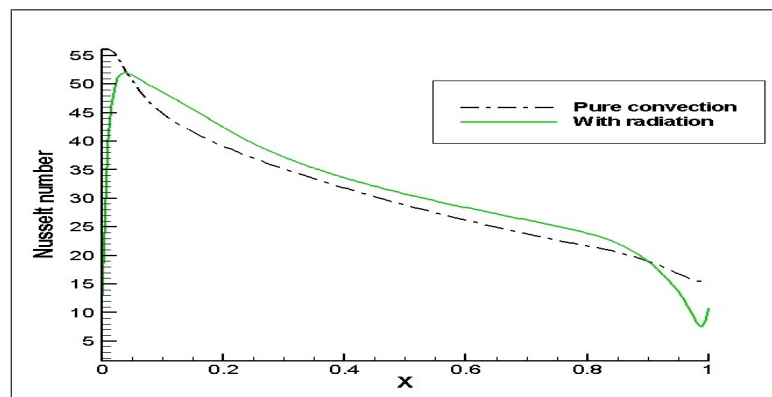
Figure 4.6: Local Nusselt number variation along heated wall for $Ra = 10^8$

4.2.1 Effect of thickness

For $Ra = 10^7$ study was carried out for different thicknesses 0.1 mm, 1 mm and 10 mm. The effect of thickness on non dimensional temperature at mid height is plotted as shown in the figure. 4.7. From the figure we can observe that the temperatures at mid height are decreasing as the thickness is increasing from 0.1 mm to 10 mm. From governing equations it is clear that the temperatures of wall depend on various parameters like thermal conductivity, surface properties like emissivity, density, heat capacity so depending upon choice of parameters the temperatures are affected. In this case as the thickness increases the rise of temperature due to conduction is lesser than decrease of temperature due to internal energy effects hence decrease in the temperature.
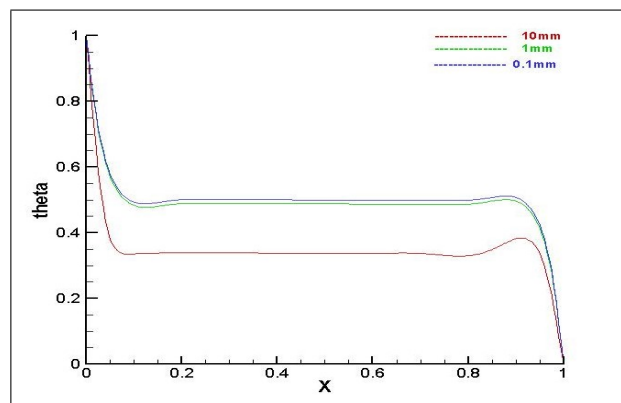
Figure 4.7: Effect of thickness on non dimensional temperature at mid height for $Ra = 10^7$

4.2.2 Effect of conduction

The governing equation for radiation involves conduction term. The study has been carried out with and without this term for square enclosure case with $Ra = 10^7$. The results shows that the temperatures at top and bottom wall are affected but there is no much variation inside enclosure. The plots for bottom and top wall non dimensional temperatures are as shown in the figure. 4.8 and 4.9. The temperatures near hot wall tends to decrease while temperatures near cold wall increase when conduction is considered which is in well accordance with the physics.
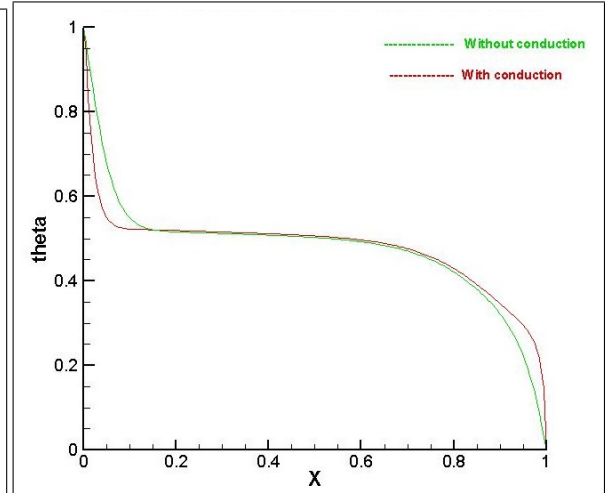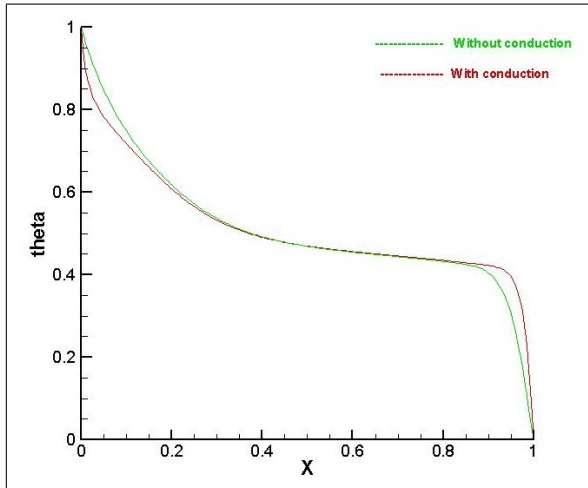
Figure 4.8: Temperatures at top wall.   Figure 4.9: Temperatures at bottom wall.

4.3   Results for partial enclosures

4.3.1   Results for parital enclosure for $Gr = 10^8$

Thermal plume behavior

For the case of partial enclosure the thermal plume behavior for pure convection and convection with surface radiation is shown in the figure. 4.10 and figure. 4.11.
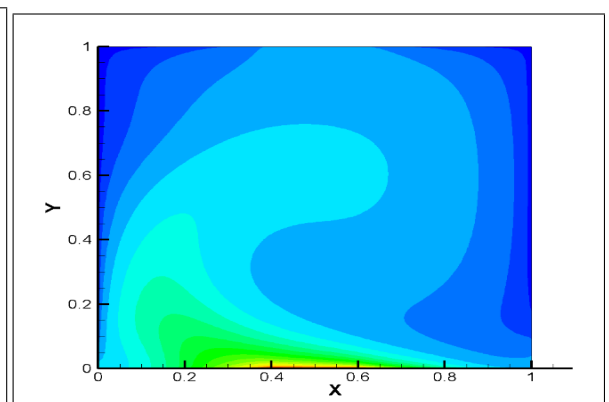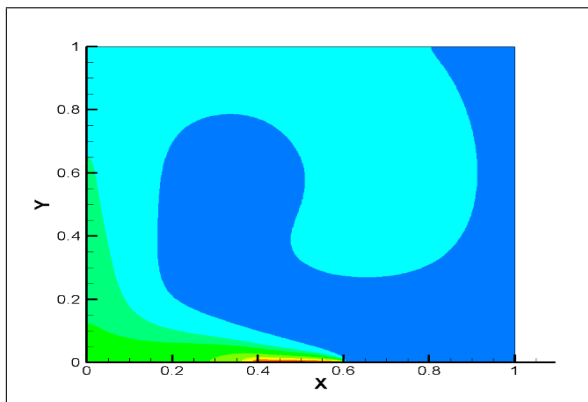


Figure 4.10:   Temperature contour with pure convection.

Figure 4.11: Temperature contour for convection with radiation.

From the contours we can infer that when we include radiation the wall temperatures are lower and more uniform throughout enclosure as compared to the wall temperatures with the pure convection. In pure convection the wall temperatures shows asymmetrical behavior with higher temperatures on the side where the plume has deviated whereas in case of radiation there is decrease in asymmetry of temperature distribution along the wall.

streamlines behavior

The streamline contours for the pure convection and convection with radiation is as shown the figure. 4.12 and figure. 4.13
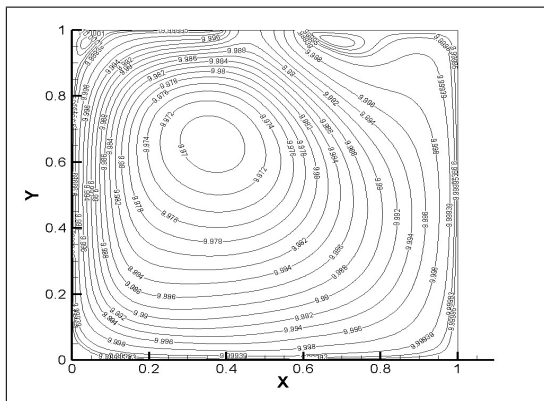
Figure 4.12: Streamline contour with pure convection.
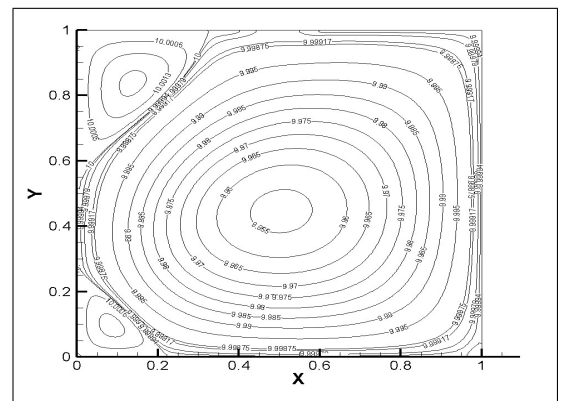
Figure 4.13: Streamline contour for convection with radiation.

As a result of larger temperature difference between wall temperature and fluid temperature in case of Radiation a unicell flow pattern with larger secondary vortices at corner is observed. Hence there are higher velocity levels in convection with radiation.

Temperature plots comparison

The mid height temperature plot for pure convection and convection with radiation is as shown in the figure. 4.14
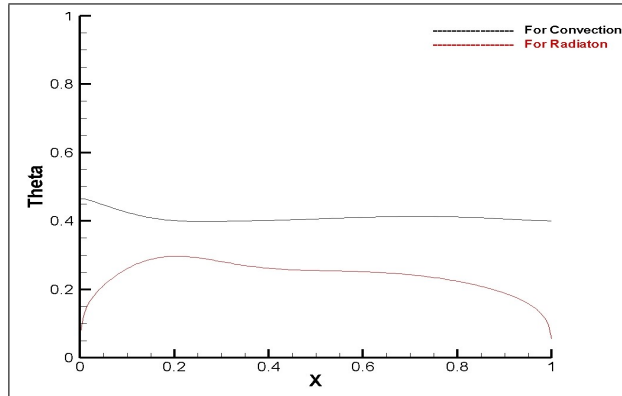
Figure 4.14: Temperature at mid height for $Gr = 10^8$

From the temperature plot it is seen that the temperatures at mid height are lower in case of convection with the surface radiation. It is because the wall temperatures are lower and same effect is propagated throughout the enclosure.

Nusselt number variation on the hot wall

The variation of Nusselt number on hot wall is as shown in the figure. 4.15. From the Nusselt number plot we can see that the Nusselt number variation is more uniform with the pure convection case and in case of convection with the radiation there is a stiff rise in the Nusselt number towards one end.
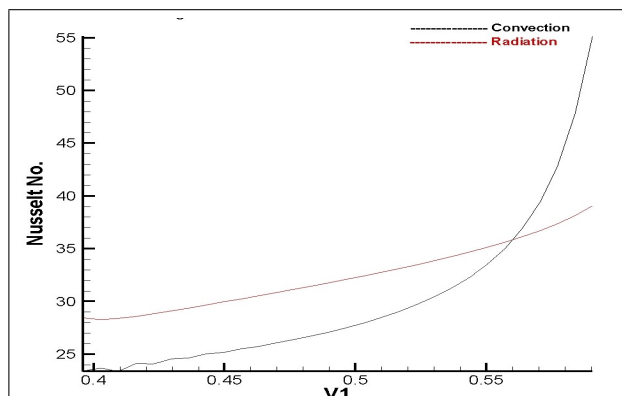
Figure 4.15: Nusselt number variation on the hot wall for $Gr = 10^8$

4.4   Parametric study for partial enclosure cases

4.4.1   Effect of the Grashof number

The study has been carried out for three different Grashof numbers namely $10^8, 10^9, 10^{10}$. This section explains the effect of Grashof number on the heat transfer characteristics of the flow. The wall material selected for the study is Iron and the thickness of wall is taken to be 10 mm. The temperature difference for Grashof numbers $10^8, 10^9, 10^{10}$ is taken as 10 C, 20 C, 30 C respectively. Figure. 4.16 shows the mid height temperature comparison between these three Grashof number.
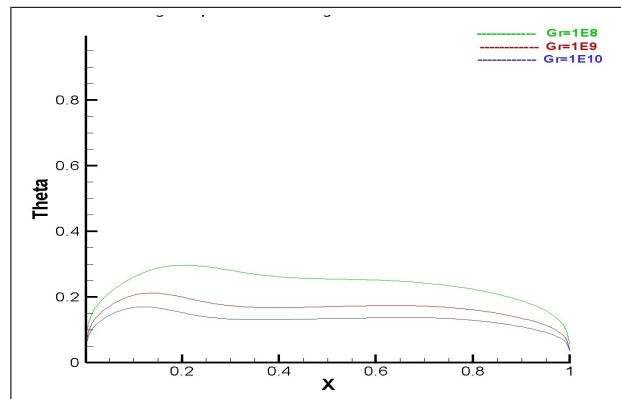
Figure 4.16: Mid height temperatures for $Gr = 10^8, 10^9, 10^{10}$

As Grashof number is increased the buoyancy force is increased in this study because of higher temperature difference. Higher buoyancy force increases flow velocity and mixing. Therefore it is seen that the temperatures at a particular location are decreasing with increase in the Grashof number. Also with the increase in the Grashof number the turbulence increases and because of more mixing there is lesser temperature gradient inside the enclosure and hence the lesser temperatures. Hence in the temperature contour plots we can see that the overall temperature levels are lesser in higher Grashof number flows. This can also be seen from the temperature contours plot 4.17 and 4.18.
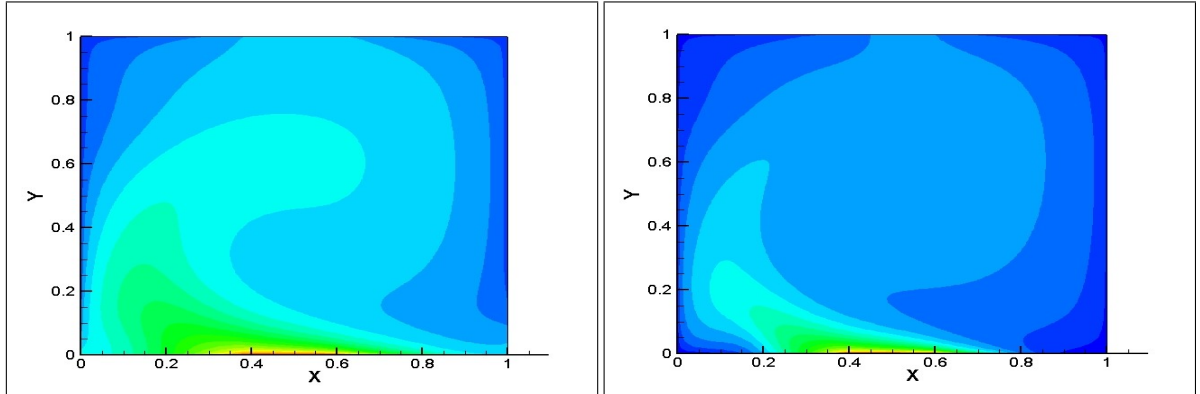
Figure 4.17: Temperature contour for $Gr = 10^8$

Figure 4.18: Temperature contour for $Gr = 10^9$.

The local convective Nusselt number variation on heated wall is as shown in the figure. 4.19.
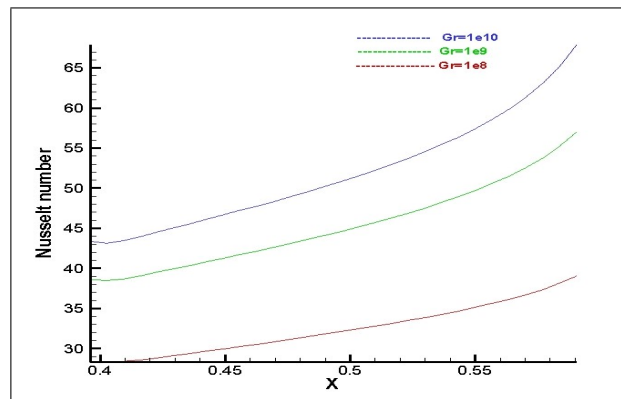

Figure 4.19: Hot wall Nusselt numbers for $Gr = 10^8, 10^9, 10^{10}$

As discussed earlier temperatures are lower for high Grashof number, which increases the value of local Nusselt numbers as shown.

4.4.2 Effect of thickness

The study was carried out for two different thicknesses $1mm, 10mm$ and Grashof number=10^8. The mid height temperature plot is as shown in the figure.4.20
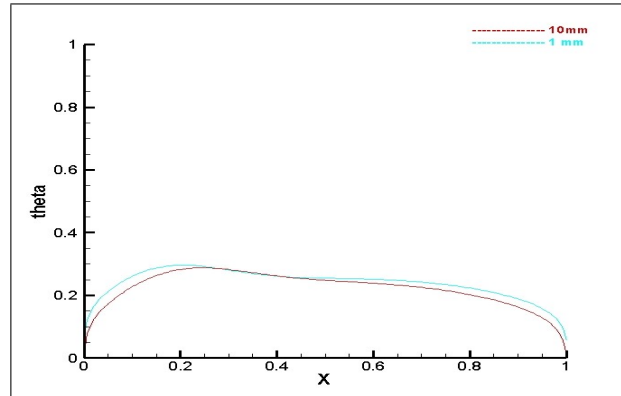
Figure 4.20: Mid height temperatures for thicknesses $= 1mm, 10mm$

It is observed that the mid height temperatures are lesser in case of 10mm wall thickness. Iron was selected for wall material. The parameters that govern the wall temperatures are conduction, convection, internal energy and radiation. As we have seen earlier that the wall temperature effects are propagated inside the enclosure. As the thickness of the wall material increases the conduction increases which tend to increase the temperature of wall. Also as thickness increases the volume of wall increases there by increasing the mass and decreasing the temperature rise for same internal energy. Between these two opposing effects depending on which one is higher the temperatures are affected. The local convective Nuselt number along hot wall is plotted as shown in the figure.4.21.
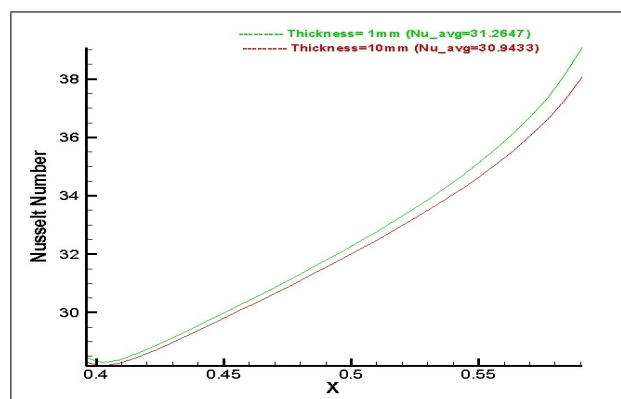

Figure 4.21: Local convective Nusselt number over hot wall for thicknesses $1mm, 10mm$

From local Nusselt number plot it is seen that the local convective Nusselt number is higher in case of lower thickness case.

4.4.3 Effect of material

The materials that were selected for the study were Iron which represents a good thermal conductor with lower emissivity value, concrete a practical building material and Plaster of Paris a insulator with higher emissivity value. The study was carried for a fixed value of Grashof number $= 10^8$. The properties of materials used are as shown in the table 4.2. These values are taken from heat and mass transfer data book by Kothandaraman *et al.* [24].

Table 4.2: Properties of the materials

Material	Iron	Concrete	POP
Density(Kg/m^3)	7870	2300	880
Thermal conductivity (W/mk)	72	1.27	0.1185
Heat capacity(J/KgK)	450	880	1090
Emissivity	0.61	0.9	0.9

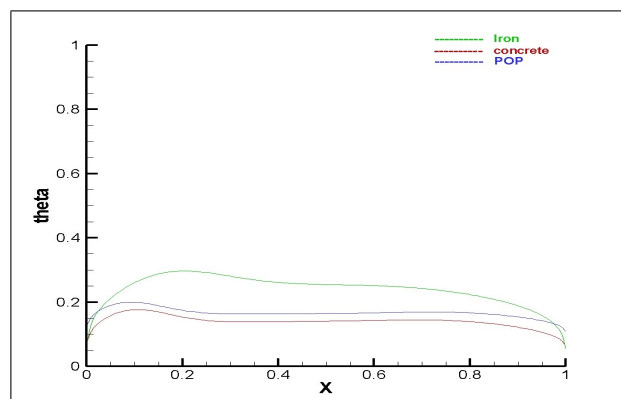The temperature plot for these materials at mid height is as shown in the figure. 4.22

Figure 4.22: Mid height temperature plot for different materials Iron, Concrete, POP at $Gr = 10^8$

From the figure we can see that the temperatures at a particular location are higher for Iron and then comparable for Concrete and POP. Approximately the temperatures of the POP are than that of the concrete. If we compare the gradient of temperature along the wall for these materials the value of gradient is higher for Iron then concrete

and POP with the least gradient. This variation of temperature shows similar trend for wall temperatures as well. This is because thermal conductivity of Iron is considerably higher than that of the concrete and POP. The local convective Nusselt number over hot wall is shown in the figure. 4.23.
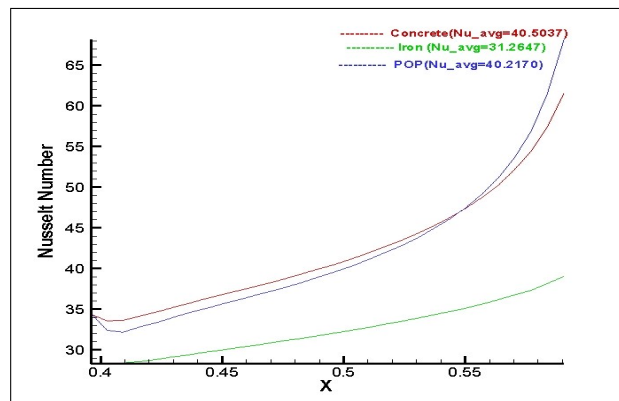

Figure 4.23: Local convective Nusselt number over hot wall for different materials Iron, Concrete and POP

From the figure we can see that the local convective Nusselt number at any point over hot wall is highest for Concrete then POP and last is Iron.

The following table.4.4.3 shows the values of average Nusselt number for different cases of flow inside partial enclosure with Grashof number varying from 10^8 to 10^{10} and for different materials like Iron, Concrete and POP.

Table 4.3: Nusselt numbers for different materials for different Grashof numbers

Gr.No.	Convection	Radiation(Iron)		Radiation(Concrete)		Radiation(POP)	
		Nu_{conv}	Nu_r	Nu_{conv}	Nu_r	Nu_{conv}	Nu_r
10^8	28.7950	31.260	17.313	40.50	28.16	40.21	26.94
10^9	40.1343	43.670	27.85	50.98	43.10	50.94	41.79
10^{10}	61.3973	49.98	52.39	55.14	79.13	55.63	78.05

Chapter 5

Train fire analysis using Fire Dynamics Simulator

5.1 Problem definition

For this part of the study train fire analysis is done. In country like India where the trains are crowded and if fire occurs the smoke and fire spread will threaten the safety of passengers. It is important to study the fire spread in train and provide safety measures, safe evacuation plans and avoid loss of property of passengers. A typical train of 20m, 3.2m, 2.6m is studied. The effect of moving train with speed 65 Kmph on fire propagation, smoke spread, temperatures at different locations will be the objective of this study. The geometry of the train is as shown in the figure.5.1. The details of the contents of the train are given in the table.5.1.The contents and geometry are with reference to [25].
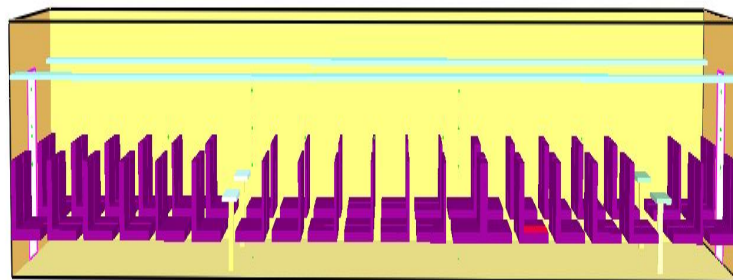

Figure 5.1: Geometry of the train [25]

Table 5.1: Combustibles inside the train compartment [25]

Item	Material	Number	Size
Chairs	Upholstery	20	$0.8 \times 0.55 \times 0.1$
Tables	Spruce	4	$0.7 \times 0.4 \times 0.5$
Table stands	Plastic	4	$0.1 \times 0.1 \times 0.75$
Shelves	Plastic	2	$20 \times 0.4 \times 0.05$
Chair backs	Upholstery	20	$0.7 \times 0.55 \times 0.1$
Flooring	Carpet	1	20×3.2

5.2 CFD model for Train fire analysis

The train fire is studied by using Computational Fluid Dynamics method. CFD software used for the study was Fire Dynamics Simulator (FDS). The model of FDS which is developed at Building and fire Research laboratory, NIST is used [26]. Two different approaches can be used to model turbulence namely FDS and LES out of which LES approach is used here [27]. The combustion model is classified in two types based on the grid size. For fine grid, DNS is used where the diffusion of fuel and oxygen is calculated for each step where as for coarse grid the LES model is used where mixture fraction combustion model is used. The mixture fraction combustion model [26] assumes that for each step at any location there exists a mixture fraction which represent the combustion parameter instead of individual species and their diffusion like in DNS. The basic assumption involved in this model is the rate of reaction is infinite and at any point of time there only exists mixture fraction. The reason for this assumption being differing time scales for convection and chemical reactions. As compared to time scale of chemical reactions the time scale of convection is very high leading to our assumption of infinite reaction rate. If $f(x, t)$ is mixture fraction at any point and at any time the conservation law gives following equation 5.1

$$\frac{\partial \rho f}{\partial t} = -\nabla.(\rho u f) + \nabla.(\rho D \nabla f) \tag{5.1}$$

From above equation mixture fraction will be obtained and from mixture fraction with states relationship mass fraction of oxygen is obtained. This mass consumption of oxygen m_o is directly praportional to heat release rate q at any location and at any point of time.

$$q = m_o H_m \tag{5.2}$$

where, H_m is heat released per unit mass of oxygen.

The train geometry is explained in the introduction. The initial conditions for train fire analysis are taken as followed, All the materials initially are at ambient except a heat source.The walls of train are treated inert except the flooring which is made up of mat and takes part in combustion. The doors are treated as open and accordingly dynamic pressure value are set depending on whether the train is moving or stationary. The pressure boundary condition is given by the following relation 5.3

$$p = \frac{\rho v^2}{2} \tag{5.3}$$

The heat source with 250 KW heat release rate is taken.

5.3 Results and Discussions

5.3.1 Validations

For the validations train fire case same as that of [25] was run and heat release rates were compared as shown the figure.5.2.
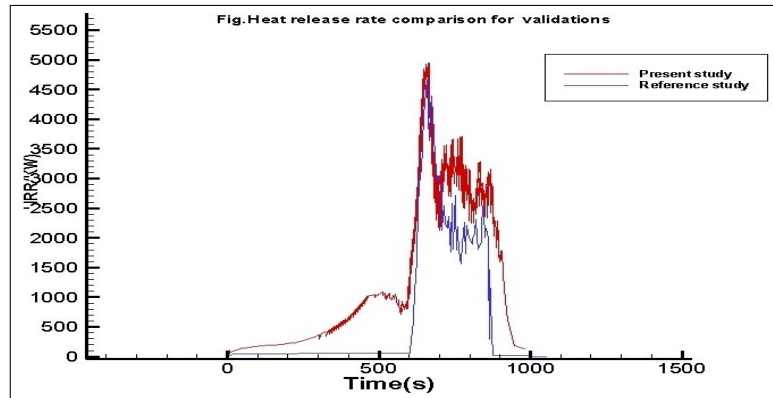
Figure 5.2: Geometry of the train

The maximum heat release rate obtained for the present study was 4782 KW which was matching with the reference value of 4.8 MW. The time for which the fire spread was there was also approximately equal.

5.3.2   Flame propagation

Flame propagation for stationary and moving train is plotted in the figure at different times as shown in the figure.5.3 to figure. 5.10
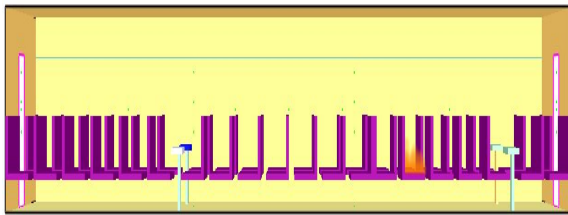

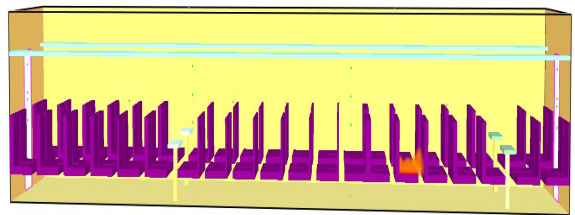Figure 5.3: Stationary train $t = 9s$ Figure 5.4: Moving train $t = 9s$
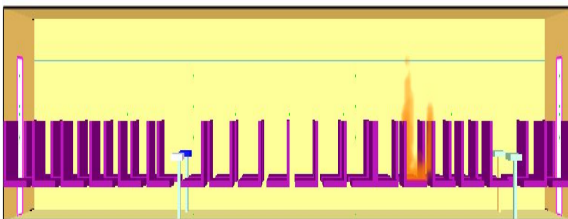

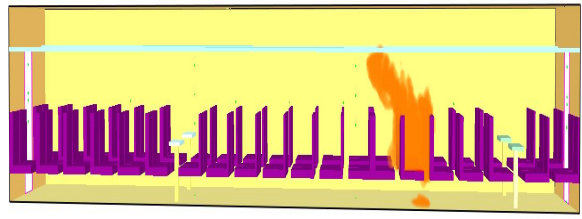
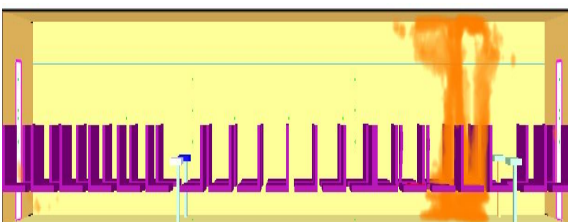Figure 5.5: Stationary train $t = 243s$ Figure 5.6: Moving train $t = 189s$
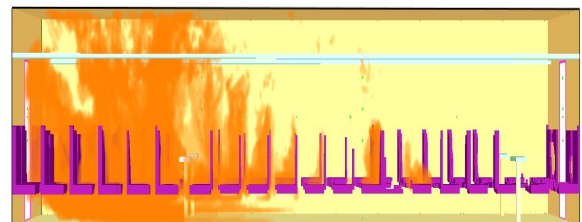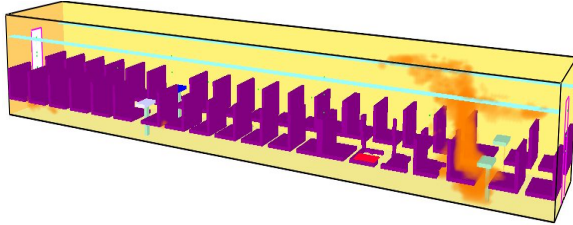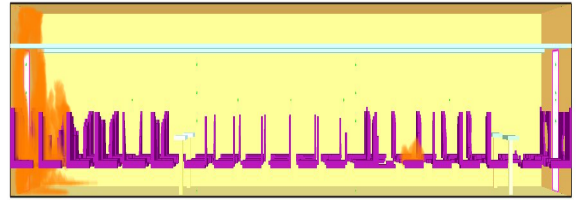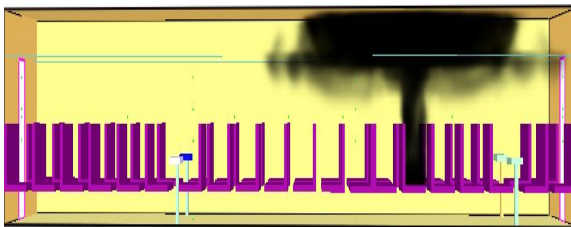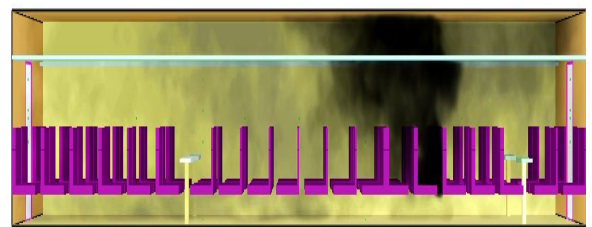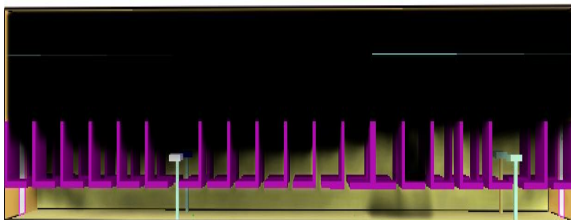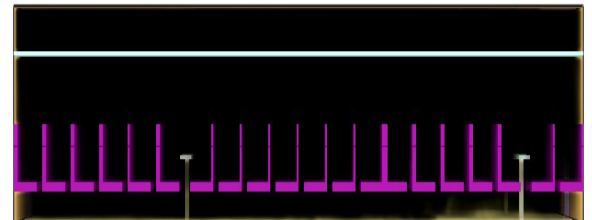

Figure 5.7: Stationary train $t = 715s$ Figure 5.8: Moving train $t = 567s$

Figure 5.9: Sattionary train $t = 835s$ Figure 5.10: Moving train $t = 657s$

From the figure it is seen that in moving train the flame propagation is in the direction of air flow and is faster as compared to the stationary train.

5.3.3 Smoke propagation

Smoke propagation for stationary and moving train is plotted at different times as shown in the figures.5.11 to 5.18.

Figure 5.11: Stationary train $t = 9s$ Figure 5.12: Moving train $t = 9s$

Figure 5.13: Stationary train $t = 243s$ Figure 5.14: Moving train $t = 189s$

Figure 5.15: Stationary train $t = 715s$
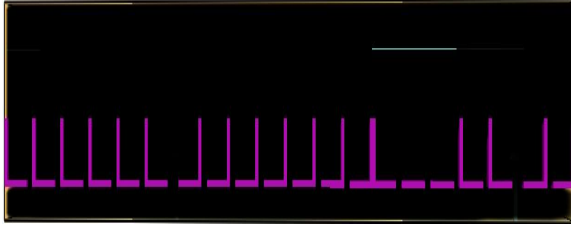

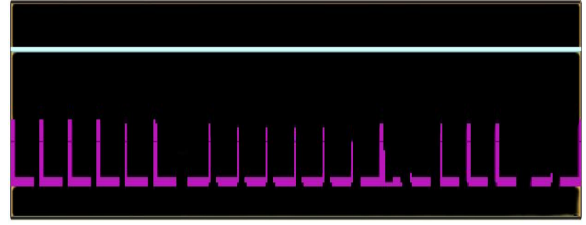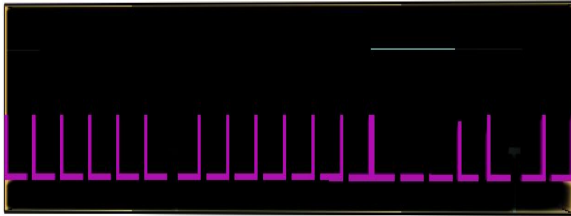Figure 5.16: Moving train $t = 567s$

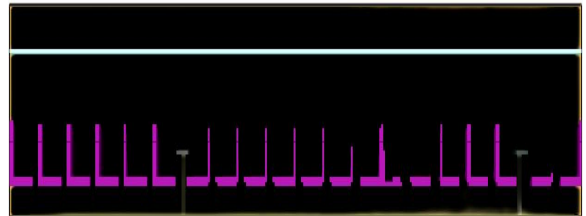Figure 5.17: Sattionary train $t = 835s$

Figure 5.18: Moving train $t = 657s$

From the figure it is seen that in moving train the smoke propagation is faster and reaches bottom in short time affecting visibility as compared to the stationary train.

5.3.4 Heat release rate

The heat release rate plot is compared for the stationary and moving train in the figure.5.19.
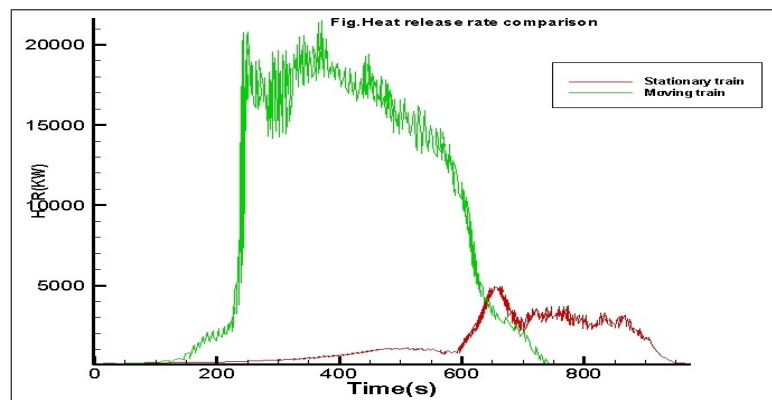

Figure 5.19: Geometry of the train

From the figure it is seen that the heat release rates in case of moving train are significantly higher than that of the stationary train. Also, for the moving train the heat release rates are significant in the time interval of 210 to 600 seconds and for stationary train it is 600 to 850 seconds. The maximum heat release rate obtained for the moving train is 21.514 MW and for stationary train it is 4.78 MW.

5.4   Temperatures at different locations

Temperatures at four locations inside train compartment were compared for the case of moving and stationary train.These locations are as follows A-Outlet door, B-6.45 m from the outlet door, C-12.45 m from the outlet door, D-Inlet door. The temperatures were recorded at 1.5 m from the floor. Figure.5.20 shows the temperature comparison at inlet and outlet doors whereas figure.5.21. shows the temperature comparison at B and C.
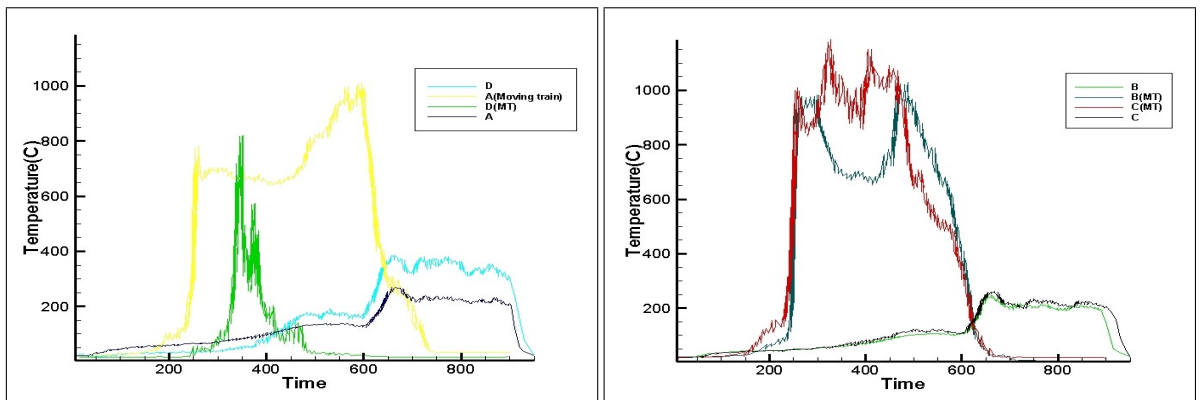
Figure 5.20: Temperature comparison at A and D

Figure 5.21: Temperature comparison at B and C

It is seen that in case of moving train temperatures are significantly higher than stationary train case at all locations.This is because supply of fresh air is higher in moving train which enhances heat release rate and fire spread. The temperatures at inlet door are higher than that of outlet door in case of stationary train. For moving train temperatures at outlet door are higher than at inlet door. The maximum temperatures reached are 412 C and 1177 C for stationary and moving train respectively. The temperatures at mid section are higher than that at doors and are of order 1000 C for moving train 200 C for stationary train for maximum time.

5.5   Smoke layer height

Smoke layer height for stationary and moving train is compared at 4 m and 8 m in the
figure.5.22 and figure.5.23 respectively.

Figure 5.22: Smoke layer height at 4 m   Figure 5.23: Smoke layer height at 8 m

The smoke layer height for stationary train increases gradually whereas for moving
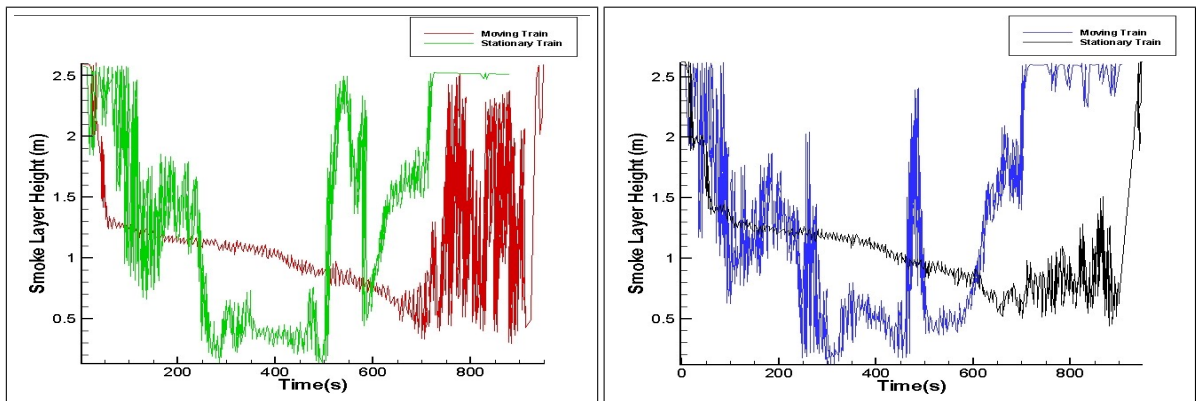train its variation with respect to time is uneven. Smoke reaches floor at around 300
seconds for moving train whereas for stationary train it takes 700 seconds.

The time taken for the burnout for stationary train was 950 seconds and that for
moving train was 740 seconds. The level of threat and damage in case of moving
train is severe. In between 600 to 850 seconds for stationary train there exists high
HRR, higher temperatures and lesser visibility. For stationary train this range is in
between 210 seconds to 600 seconds. Hence safe time for evacuation is 0-400 seconds
for stationary train and 0-150 seconds for moving train. Human being cannot sustain
temperatures greater than 100 C even for few minutes and die if they breathe air of
temperature greater than 60 C. The smoke contains carbon monoxide, which when
inhaled reacts with haemoglobin present in the blood and forms carboxyhaemoglobin
which reduced the oxygen carrying capacity of the blood. Two third of the total deaths
in fire accident are not because of fire exposure but because of toxicity of smoke [28].
Out of which maximum deaths occur far away from the heat source.

Chapter 6

Conclusions

The following conclusions are drawn from the study

- The effect of radiation significantly alters the plume characteristics as well as heat transfer rate.

- The temperature decreases in the enclosure compared to convection due to increase of heat transfer rate with convection and radiation.

- With Radiation wall temperature exhibit symmetrical behavior and same nature of solution is propagated inside the enclosure (Because of Conduction and Radiation).

- Because of reduction in wall temperatures in case of convection with surface radiation there is increases in the magnitude of natural convection velocity and turbulence levels at boundary layers indicated by higher value of maximum streamline function. This has increased convective heat transfer significantly.

- In case of convection with radiation a unicell flow pattern with larger secondary vortices at corner is observed .

- The average convective and radiative Nusselt number increases with increase in Grashof number.

- As the thickness of the wall decreases there is higher convective heat transfer and hence average convective Nusselt number increases in case of convection with radiation for Iron.

- The average convective Nusselt number and hence heat transfer is less for Iron as compared to concrete and POP whose values are comparable.

- Threat level in case of moving train fire with doors open is very severe.

- Heat release rate curves shows stiff increase at the beginning and hence immediate fire suppression systems should be designed and placed in the compartment to avoid damage.

- The smoke spread is the source of hazard and based on the smoke spread study the smoke exhaust systems should be placed at top wall and located at two ends to keep the smoke high.

References

[1] G. D. Mallinson, G. De Vahl Davis, "Three-dimensional natural convection in a box-a numerical study", *J. Fluid Mech. 83, 1-31*, 1977.

[2] G. De Vahl Davis, "Natural convection of air in a square cavity: a bench mark numerical solution", *Internat. J. Numer. Methods Fluids 3, 249-264*, 1983.

[3] Tanmay Basaka, S. Royb, A. R. Balakrishnana, "Effects of thermal boundary conditions on natural convection flows within a square cavity", *International Journal of Heat and Mass Transfer 49(23), 4525-4535*, 1983.

[4] N. C. Markatos and K. A. Pericleous, " Laminar and turbulent natural convection in an enclosed cavity", *Int. J. Heat Mass Transfer 27, 755-772*, 1984.

[5] Y. S. Tian, T. G. Karayiannis, "Low turbulence natural convection in an air filled square cavity part I: the thermal and fluid flow fields", *Int. J. Heat Mass Transfer 43, 849-866*, 2000.

[6] H. N. Dixit, V. Babu, "Simulation of high Rayleigh number natural convection in a square cavity using the lattice Boltzmann method", *newblock Int, J. Heat Mass Transfer 49, 727-739* , 2006.

[7] G. V. Kuznetsov, M. A. Sheremet, "Numerical simulation of turbulent natural convection in a rectangular enclosure having finite thickness walls", *Int. J. Heat Mass Transfer 53, 163-177*, 2010.

[8] G. Barakos, E. Mitsoulis, D. Assimacopoulos, "Natural convection flow in a square cavity revisited: Laminar and turbulent models with wall functions", *International Journal for Numerical Methods in Fluids 18.7, 695-719*, 1994.

[9] A. H. Abib, Y. Jaluria, "Numerical simulation of the buoyancy induced flow in a partially open enclosure", *Numer. Heat Transfer, Part A 14, 235-254*, 1988.

[10] J. Prahl, H. W. Emmons, "Fire induced flow through an opening", *Flame. 25, 369-385*, 1975.

[11] R. Harish, K. Venkatasubbaiah, "Mathematical modeling and computation of fire induced turbulent flow in partial enclosures", *Applied Mathematical Modelling 37, 9732-9746*, 2013.

[12] R. Harish, K. Venkatasubbaiah, "Numerical simulation of turbulent plume spread inside ceiling vented enclosure ", *European Journal of Mechanics B/Fluids 42, 142-158*, 2013.

[13] Ramesh. N., and S. P. Venkateshan, "Effect of surface radiation on natural convection in a square enclosure", *Journal of thermophysics and heat transfer 13.3, 299-301*, 1999.

[14] K. Velusamy, T. Sundararajan and K. N. Seetharamu , "Interaction Effects Between Surface Radiation and Turbulent Natural Convection in Square and Rectangular Enclosures ", *Journal of Heat transfer 10.1115/1.1409259*, 2001.

[15] H. Singh, S. N., and S. P. Venkateshan, ""Numerical study of natural convection with surface radiation in side-vented open cavities", *International Journal of Thermal Sciences 43.9, 865-876*, 2004

[16] H. Bouali , A. Mezrhaba, H. Amaoui , M. Bouzid, " Radiation-natural convection heat transfer in an inclined rectangular enclosure", *International Journal of Thermal Sciences 45, 553-566*, 2006.

[17] G. Lauriat , G. Desrayaud, "Effect of surface radiation on conjugate natural convection in partially open enclosures", *International Journal of Thermal Sciences 45, 335-346*, 2006.

[18] Anil Kumar Sharma, K. Velusamy , C. Balaji , Venkateshan , " Conjugate turbulent natural convection with surface radiation in air filled rectangular enclosures", *International Journal of Heat and Mass Transfer 50, 625-639*, 2007.

[19] DWESH K. SINGH , S.N. SINGH, "Conjugate free convection with surface radiation in open top cavity", *International Journal of Heat and Mass Transfer 89, 444-453*, 2015.

[20] HINOJOSA, J. F., CABANILLAS, R. E., ALVAREZ, G., ESTRADA, C.E., " Nusselt number for the natural convection and surface thermal radiation in a square tilted open cavity", *International Communications in Heat and Mass Transfer, 32(9), 1184-1192.*, 2005.

[21] MICHAEL F. MODEST, "Radiative Heat transfer (Second edition)", *Academic press, 149-152*, 2011.

[22] T. K. SENGUPTA, S. K. SIRKAR AND A. DIPANKAR, "High accuracy schemes for DNS and acoustics", *J. Sci. Comput. 26 , 151-193*, 2006.

[23] K. VENKATASUBBAIAH, T. K. SENGUPTA, "Mixed convection flow past a vertical plate: Stability analysis and its direct simulation", *Int. J. Therm. Sci. 48, 461-474*, 2009.

[24] C. P. KOTHANDARAMAN, S. SUBRAMANYAM, "Heat and mass transfer data book (Eighth edition)", *New age international (p) Ltd., 1-34* , 2014.

[25] W. K. CHOW, K. C. LAM, N. K. FONG, S. S. LI, Y. GAO, "Numerical Simulations for a Typical Train Fire in China, Modelling and Simulation", *Engineering Volume 2011, Article ID 369470, 7 pages* , 2011.

[26] KEVIN MCGRATTAN, RANDALL MCDERMOTT, SIMO HOSTIKKA, JASON FLOYD, "Fire dynamics simulator (Version 5)", *Fire Research Division, Building and Fire Research Laboratory, National Institute of Standards and Technology, Gaithersburg, Md, USA*, 2010.

[27] K. B. MCGRATTAN, H. R. BAUM, AND R. G. REHM, "Large Eddy Simulations of Smoke Movement", *Fire Safety Journal, vol. 30, no. 2, 161-178*, 1998.

[28] MO SHAN-JUNA, LI ZI-RONGA, LIANG DONGA, LI JIA-XINA, ZHOU NAN-JIANGA, "Analysis of Smoke Hazard in Train Compartment Fire Accidents Base on FDS", *Procedia Engineering 52, 284-289*, 2013.